New Method for Silicon Nitride Synthesis Via Hybrid Polymer Nanocomposites

ANITA-LAURA RADU[1*], ANDREI SARBU[1], STEFANIA MOTOC[2], LUMINITA MARA[3], VICTOR FRUTH-OPRISAN[4], SORINA ALEXANDRA GAREA[5], STEFAN OVIDIU DIMA[1], GHEORGHE NECHIFOR[5], LILIANA SARBU[1], HORIA IOVU[5]

[1] National Research and Development Institute for Chemistry and Petrochemistry-ICECHIM, Polymers Department, 202 Independentei Spl., Bucharest, Romania

[2] Metallurgical Research Institute,060021, Bucharest, Romania

[3] National Research-Development Institute for Nonferrous and Rare Metals-IMNR, Pantelimon, Romania

[4] Romanian Academy, Physical Chemistry Institute "Ilie Murgulescu", 202 Splaiul Independentei, 060021, Bucharest, Romania

[5] Politechnic University of Bucharest, Applied Chemistry and Material Science Faculty, 149 Calea Victoriei, 010072, Romania

Mesoporous silica was obtained by the acid attack of a serpentinite rock. This material was soaked with acrylonitrile (containing azobisisobutyronitrile as initiator) and the radical polymerization led to the obtaining of polymer inorganic-organic nanocomposites. The polymer nanocomposites were transformed in carbon-silica nanocomposites by the cyclization and graphitization of the carbon chain polymer. Heating the carbon-silica nanocomposite in nitrogen atmosphere allowed the synthesis of silicon nitride, a raw material for special ceramics.

Keywords: radical polymerization, nanocomposite, silica, silicon nitride

The combination of synthetic polymer characteristics (elasticity, low density and easy processing) with those of inorganic materials, such as ceramics, oxides and metals (hardness, thermal stability and large availability) opens new perspectives in material science. In recent years, an increased interest has been devoted to the preparation and application of polymer/inorganic nanocomposites, which has been pursued as a route to combine the advantageous properties of the nanometer materials, inorganic compounds and polymer into one material [1-3].

The synthesis of inorganic-organic nanocomposite materials (containing an important inorganic amount) developed especially in the last decade [4-12].

There are several methods for the inorganic-organic nanocomposite synthesis [13-18], among which the most accessible is the polymerization in inorganic nanostructures [15]. As inorganic nanostructure hosts mesoporous silica [19], zeolites [6], MCM [6], etc are used. A particular case is the acrylonitrile polymerization in sepiolite (a hallow fiber magnesium silicate), followed by the transformation of the composite in carbon-silicate nanocomposite and subsequently (by carbothermal nitridation) in silicon nitride, a raw material for advanced ceramics [20]. The carbothermal nitridation reaction can start from magnesium silicate or from silica [21, 22]:

$$3Mg_2SiO_4(s) + 2N_2(g) + 12C(s) \rightarrow Si_3N_4(s) + 6Mg(g) + 12CO(g)$$
$$3SiO_2(s) + 6C(s) + 2N_2(g) \rightarrow Si_3N_4(s) + 6CO(g)$$

In both cases, being a reaction between two solids and a gas, the intimate mixture between the two solids and the porosity of the solid phase are essential.

The present work describes some results concerning the synthesis of silica-polyacrilonitrile nanocomposites starting from a new raw material: serpentinite, a soft (Mohr hardness about 3) magnesium silicate rock resulted as sterile mass from the previous mining exploitation of asbestos and found in several dumps (which must be eliminated) in the „Portile de Fier" Natural Park, on the Danube border, in the south- west of Romania. The obtained polymer nanocomposites were subsequently used for the synthesis of silicon-nitride, a raw material for special ceramics.

The use of serpentinite as starting material for silicon nitride synthesis, via polymer nanocomposite, has several advantages over the other methods: a smaller price, the recovery of a material with little utilization, preventing the professional diseases caused by inorganic fibers, the cleaning of a natural park.

Experimental part

Materials

Serpentinite from Dubova (Romania) dumps was an offer from Dubova Mineral Prod. Com. SRL- Romania. Hydrochloric acid 6M, azobisisobutyronitrile (AIBN) and acrylonitrile (AN), were purchased from Fluka, and were of analytical degree. AN was desinhibited by rectification.

Polymer nanocomposites and silicon nitride synthesis

The serpentinite from dumps was grounded and attacked with concentrated mineral acid: HCl 6M, at 4.6 vol/wt ratio and various temperatures and reaction times. A silica gel and a liquid were produced, which were separated by filtration. The silica gel was washed with water and dried yielding a grey silica powder.

The silica powder was soaked with acrylonitrile (containing the azobisisobutyronitrile as radical initiator) in an ampoule and the oxygen was eliminated by purging with a low flow of nitrogen. Then the ampoule was closed and its bottom was introduced in an ultra thermostat water bath having 65 °C. In these conditions the polymerization of acrylonitrile within the silica pores occurred.

The polymer composite was heated at 2 temperatures: 300 °C in air and 550 °C in inert atmosphere in order to get a silica-carbon porous nanocomposite.

The carbothermal nitridation occurred in a Tammann oven with graphite resistance, in nitrogen flow, at 1400-1500 °C.

* *email: raduanita@yahoo.com; Tel: 0723599783*

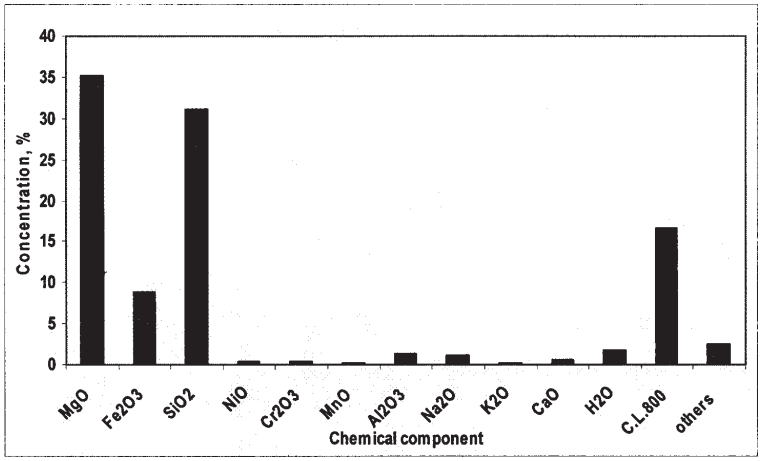

Fig. 1. The average chemical composition of serpentinite rocks from dumps
Note: C.L.800 means the calcinations losses at 800 °C

Analysis

The serpentinite was checked for chemical and mineralogical composition and granulation. The silica was analyzed concerning the chemical composition, size, density, specific surface, pore dimension and morphologic structure. The polymer inorganic-organic nanocomposites were analyzed by FTIR, DTA/DTG, TEM and SEM. The silica-carbon nanocomposites and the silicon nitride were analyzed by XRD.

Granulometry was recorded by sieving.

The particle size was detected in glycerol suspensions by dynamic light scattering with a zetasizer (Nano-ZS from Malvern) with a 4mW He-Ne, 633 nm lasers, which measures in the 0.6 nm- 6 μm size range.

The density was measured by Archimedes Method. The silica specific surface and pore dimension were obtained by Brunauer- Emmett- Teller method (BET). The morphologic structure was assessed by XRD (HZG-4) with the radiation CuKα1&2, by step by step scanning in the θ range 0-80 °

The DTA/TGA (TA Q500) analysis was performed at a heating rate of 10 °C/min in air and the FTIR spectra were registered from KBr pellets on a SHIMADZU 8900 Fourier Transform Infrared Spectrophotometer using 40 scans and 4 cm^{-1} resolution, in the range 500-4000 cm^{-1}. Transmission electron microscopy (TEM) observations were carried out at 100 kV (JEOL 1200 EXII). Scanning electron microscopy (SEM) observations were carried out (Hitachi S-4500) at 5 kV accelerating voltage, the samples being viewed after the deposition on the Al support and coating with Au.

Results and discussions

Serpentinite characterization

Samples of serpentinite from various dumps were collected and analyzed in order to check the chemical and mineralogical composition. The average chemical composition of the serpentinite rocks from the dumps is presented in figure 1.

As one can see from figure 1, the main components of serpentinite rocks are MgO and silica, in almost equal concentrations (about 37 %) and Fe_2O_3 (about 9 %).

The serpentinite rocks were grounded, obtaining a powder having the granulometric composition presented in table 1. Table 1 shows that, practically, all the serpentinite powder was less than 200 μm, about 60% being under 63μm.

The mesoporous silica

The acidic attack of the serpentinite powder with HCl at various reaction times (30, 60, 90 and 120 min), yielded silica with different purity shown in figure 2. In the studied range, the greatest purity was observed at a reaction time of 60 min.

The particle size of obtained silica samples are presented in figure 3. Figure 3 shows that working at the same temperature but at different reaction times, some samples are monodisperse and other polydisperse: the sample attacked at 90°C during 120 min is monodisperse (R15), but the sample attacked at 90°C during a shorter time-60 min. (R11) is polydisperse; the sample attacked at 60°C during 30 min (R9) is monodisperse, but the sample prepared at the same temperature (60°C) during a longer time- 60 min. (R3) is polydisperse.

Figure 4a displays the density and figure 4b the specific surfaces of various silica samples prepared at different temperatures and reaction times: R7 and R8 were prepared at 50°C during 60 min and respectively during 90 min.; R9 and R12 were prepared at 60°C during 30 min and respectively 90 min; R13 was prepared at 70°C during 30 min and R10, R11 and R14 were prepared at 90°C during 30, 60 and 90 min respectively. Figure 4a shows that the density of the samples varies between 1.89 and 2.00 g/cm^3, the smaller densities being observed at higher temperature and longer reaction times (sample R14). Figure 4b shows that the specific surfaces are high (generally between 350- 400 m^2/g). This is a first indication that the samples are highly porous.

Table 1
GRANULOMETRIC COMPOSITION OF SERPENTINITE AFTER MILLING

Granulometric class	+200μm	-200μm +90 μm	-90μm+63 μm	-63 μm
[%]	2.2	28.6	10.6	58.6

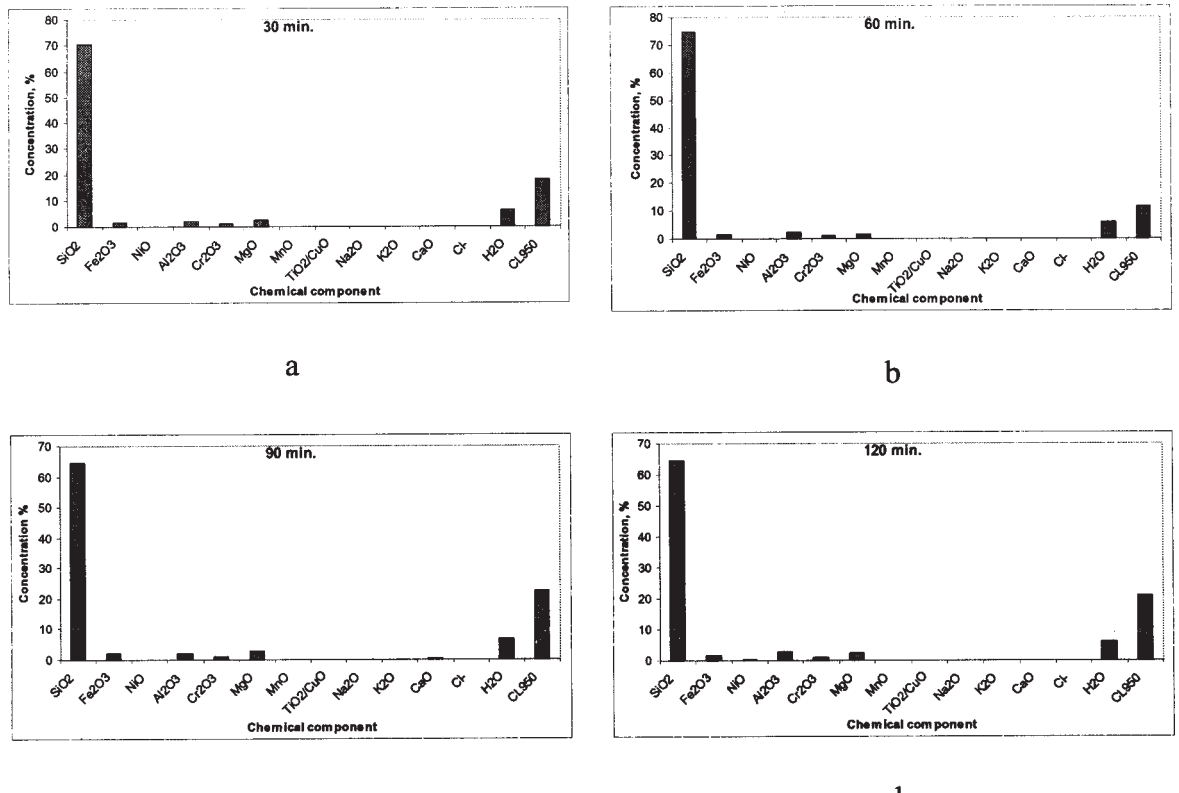

Fig. 2. The chemical composition of silica after the attack of serpentinite powder with HCl 6 M, at 90 °C, at a liquid: solid ratio of 4.6 and different reaction times: 30 (a), 60 (b), 90 (c) and 120 minutes (d); CL950 are the calcinations losses at 950 °C

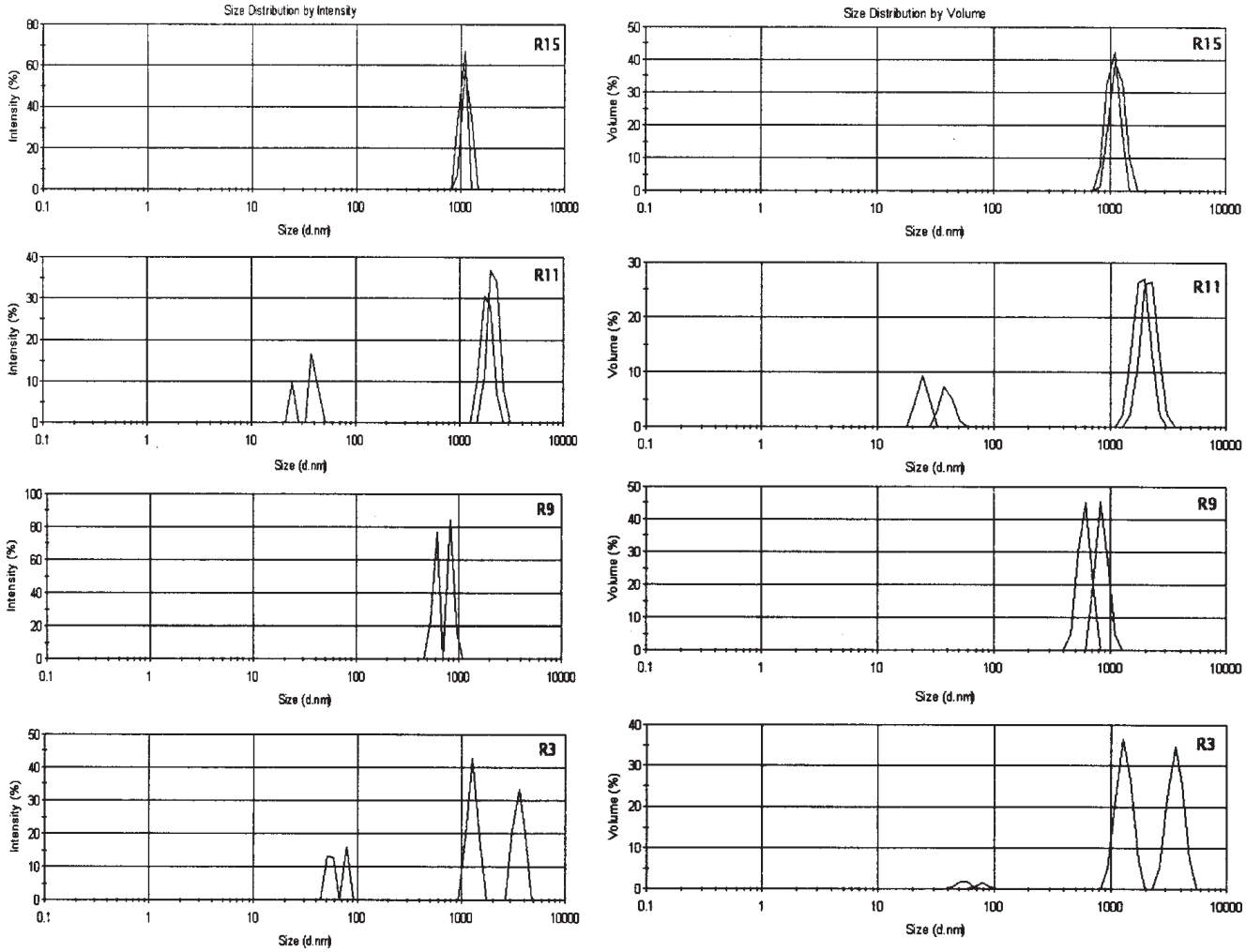

Fig. 3. Size distribution of silica particles, by intensity (a) and by volume (b), from light scattering determinations

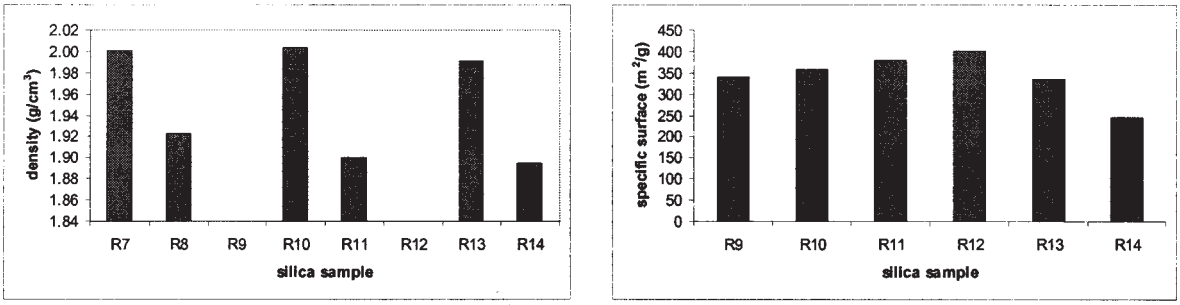

a b

Fig. 4. Density (a) and specific surface area (b) for some silica samples

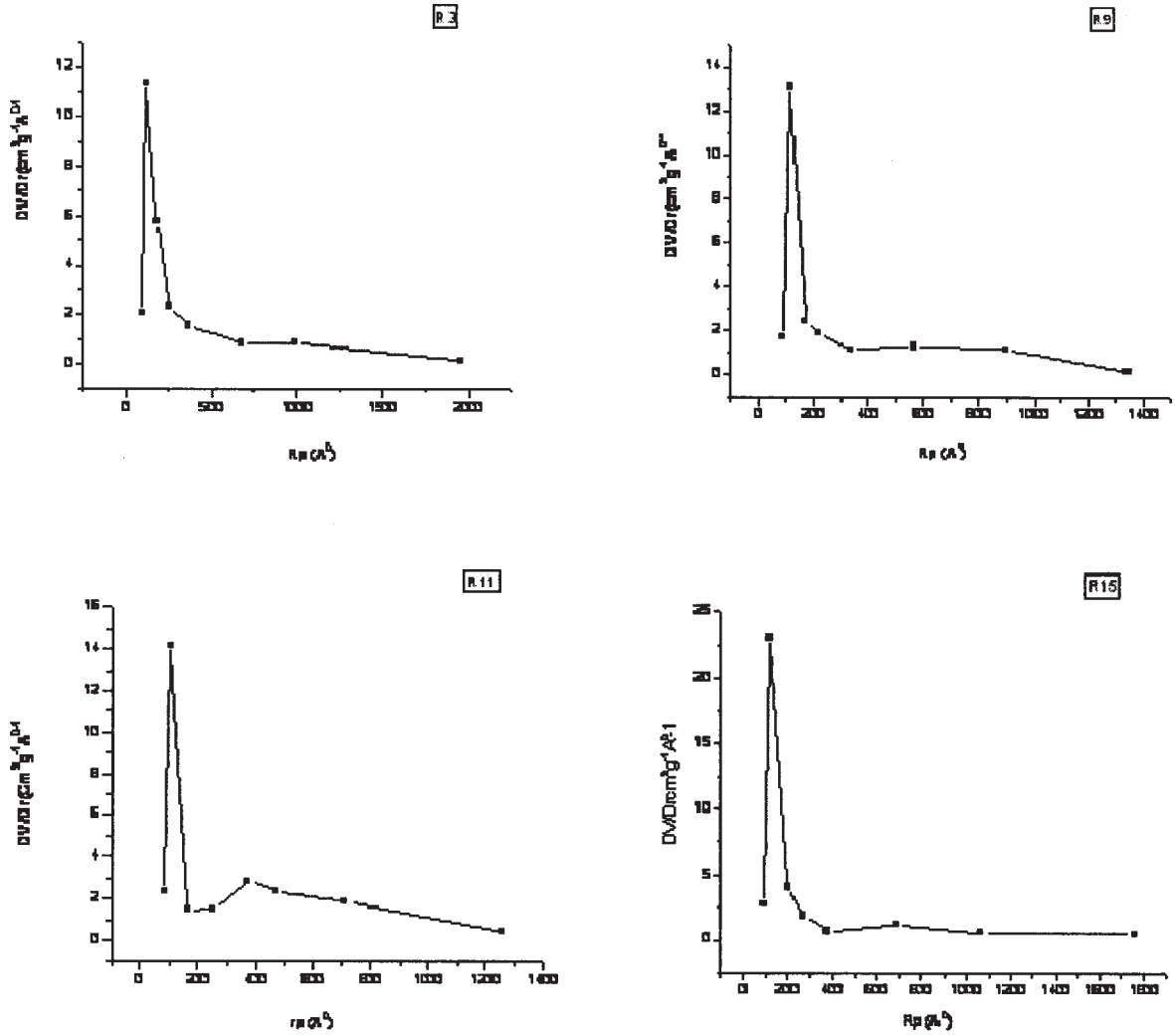

Fig. 5. Pore diameter distribution of some silica samples, calculated from BET data

Figure 5 shows the pore dimensions of silica particles, calculated from BET data. From figure 5 one can see that, independently of the acid attack conditions, the average diameter of silica pores is about 200Å (20 nm), meaning that obtained silica contains nanopores.

Figure 6 shows the XRD diffractograms for two silica samples, prepared at 60°C during 60 min. (R3) and respectively 90 min. (R12). The diffractograms are similar, revealing a highly amorphous content (over 70%) and traces of some minerals from the initial serpentinite.

The above results show that the sterile mass of serpentinite from the Dubova dumps can be valorized to mesoporous silica (pore diameter about 20 μm) by the attack with 6 M HCl.

Silica- Poly (acrylonitrile) nanocomposite

The polyacrilonitrile- silica nanocomposites were characterized by DTA/TGA, FTIR, SEM and TEM.

The figure 7a and b show the DTA/TGA curves for silica (RN 55- prepared at 90°C, 60 min) and respectively for the polymer nanocomposite obtained from it and figure 8a and b the FTIR spectra for the same samples.

The differences between the thermal behaviour of silica and polymer composite in figure 7a and respectively in figure 7b prove the formation of the new nanocomposite material. The decrease of silica sample mass till 700 °C is only about 15% for silica, but about 40% for the composite. In the same time the composite shows a quick loss of

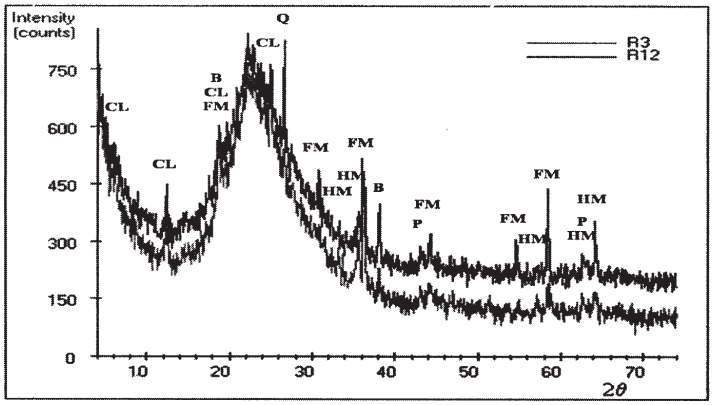

Fig. 6. Diffractograms for two silica samples, prepared at 60°C and at 60 min, (R3) and respectively 90 min. (R12) reaction times. Q – Quartz, CL – Chlorite, HM – Hematite, FM – Magnesium Ferrite / Magnetite, P – Periclase, B – Brucite

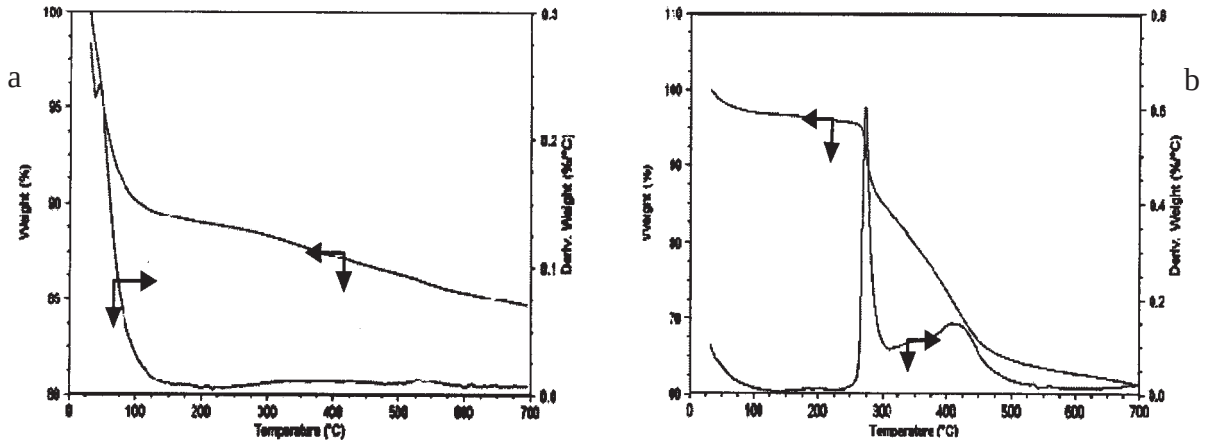

Fig.7. DTA/TGA curves for silica (a) and the correspondent polymer composite (b)

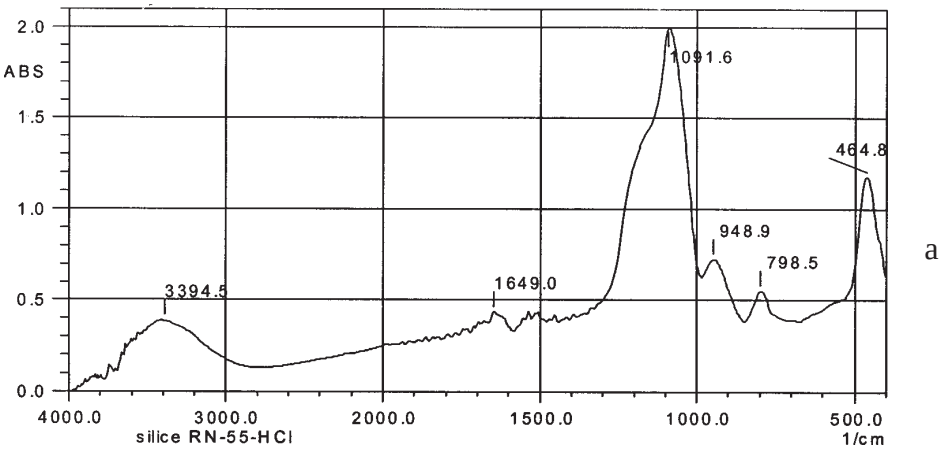

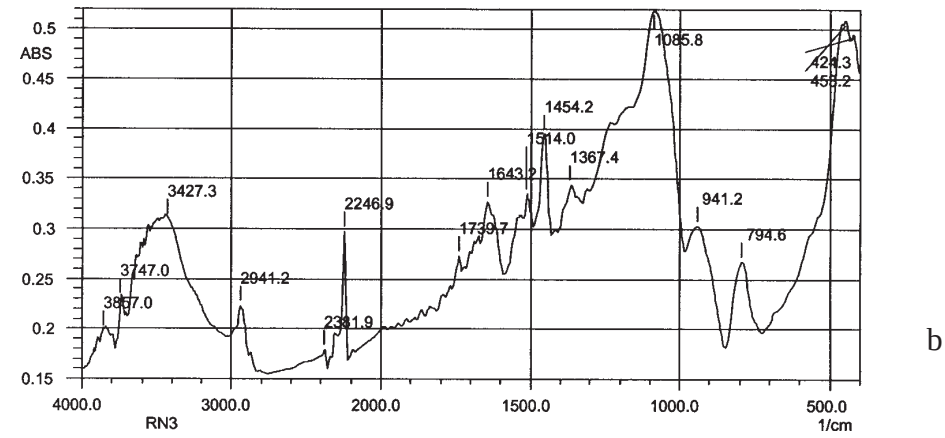

Fig. 8. FTIR spectra for silica (a) and polymer nanocomposite (b)

masses at about 280°C (probably due to the cyclization process of the polyacrylonitrile), which is not present in figure 7a for the inorganic material.

Comparing the FTIR spectra in figure 8a and b, one can see in figure 8b the presence of the CN band in the nanocomposite (at 2247 cm^{-1}) and the obvious modification of the spectra in the 1800- 1100 cm^{-1}, suggesting the formation of a hybrid inorganic- organic nanocomposite.

Figure 9 shows a TEM (a) and SEM photography (b) of a polymer- silica nanocomposite. One can see that the average pore diameters are around 20 μm (as it was also

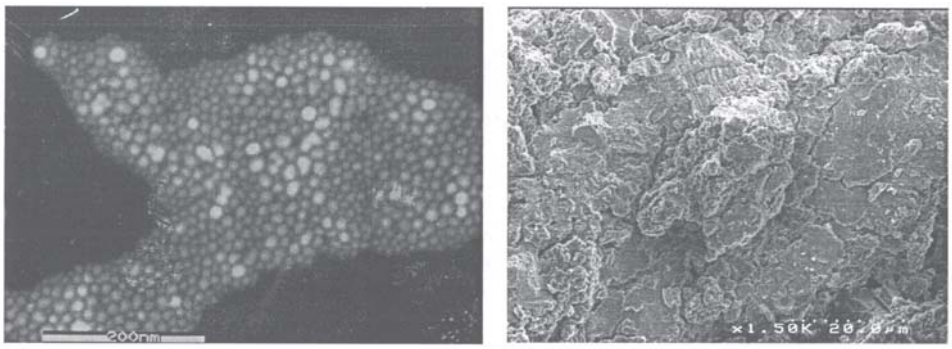

a b

Fig. 9. TEM (a) and SEM (b) photography of a polymer- silica nanocomposite

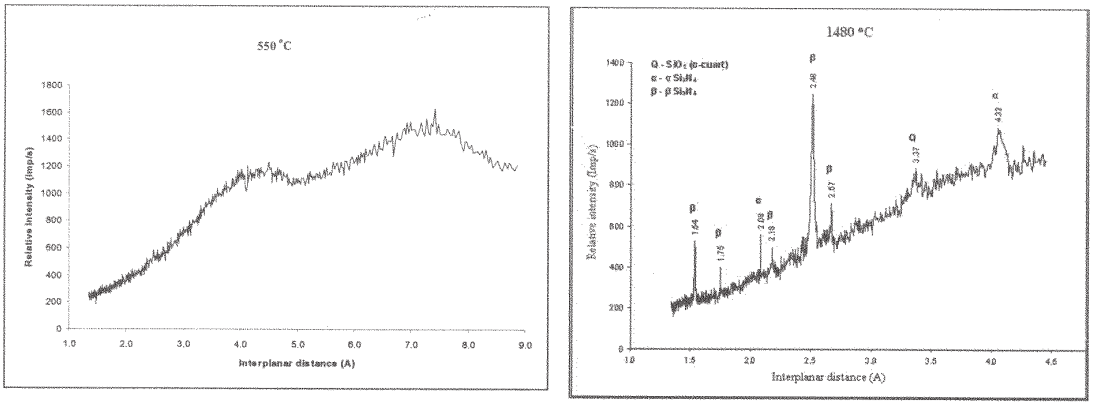

a b

Fig. 10. XRD spectra for carbon-silica-nanocomposite (a) and for the silicon nitride obtained from it by carbothermal nitridation (b)

calculated from BET data), some of pores being filled and others unfilled with polymer.

Silica- carbon nanocomposite and silicon nitride

Figure 10 shows the XRD spectra of the carbon-silica nanocomposite (a), obtained by the cyclization and graphitization of silica- polyacrylonitrile composite and of the product obtained after the carbothermal nitridation (b). The carbon- silica composite is amorphous and the silicon nitride is a mixture of α and β forms.

Conclusions

The serpentinite waste rocks from the Dubova dumps can be valorized to mesoporous silica (pore diameter about 20 nm) by the attack with 6 M clorhydric acid.

Performing the radical polymerisation of acrylonitrile in the mesoporous silica a hybrid polymer inorganic-organic nanocomposite is synthesised.

The polymer nanocomposite can be transformed in an amorphous carbon-silica nanocomposite, which, after the carbonitridation reaction, forms a mixture of α and β silicon nitride powder, useful for special ceramics.

References

1. BAOLI, O., DUXIN, L., Sci China Ser B-Chem., **50** (3), 2007, p. 385
2. DONESCU, D., VULUGA, Z., RADOVICI, C., SERBAN, S., Mat. Plast., **45**, nr. 4, 2008, p. 305
3. GAREA, S., CONSTANTIN, F., VOICU, G., IOVU, H., Mat. Plast. **45**, no. 4, 2008, p. 414
4. DONESCU, D., RADOVICI, C., BERCU, C., GHIUREA, M., BOSCORNEA, C., Mat. Plast., **45**, no. 1, 2007, p. 7
5. IANCHIS, R., DONESCU, D., PETCU, C., Mat. Plast., **45**, no. 3, 2008, p. 265-268, 265
6. LEBEAU, B., PATARIN, J., SANCHEZ, C., Adv. in Technol. of Mat. and Mat. Proc., **6** (2), 2004, p. 298
7. BOURGEAT-LAMY, E., J. Nanosci. Nanotech., **2**, 2002, p. 1
8. SANCHEZ, C., LEBEAU, B., CHAPUT, F., BOILOT, J. P., Adv. Mater., **15**, 2003, p. 1969
9. SANCHEZ, C., JULIAN, B., BELLEVILLE, P., POPALL, M., J. Mater. Chem., **15**, 2005, p. 3559
10. GÓMEZ-ROMERO, P., CUENTAS-GALLEGOS, K., LIRA-CANTU, M., CASAN-PASTOR, N., J. Mater. Sci., **40**, 2005, p. 1423–1428. doi: 10.1007/s10853-005-0578-y
11. HOFFMANN, F., CORNELIUS, M., MORELL, J., FRÖBA, M., Angew. Chem. Int. Ed. Eng., **45**, 2006, p. 3216
12. SANCHEZ, C., SOLER-ILLIA, G. J. D. A. A., RIBOT, F., GROSSO, D., Compt. Rend. Chim., **6**, 2003, p. 11311
13. SAMUNEVA, B., KABAIVANOVA, L., CHERNEV, G., DJAMBASKI, P., KASHCHIEVA, E., , EMANUILOVA, E., SALVADO, I. M. M., FERNANDES, M.H.V, WU, A., J. Of Sol-Gel Sci. And Techn., **48** (1-2), 2008, p. 73
14. CHOW, P.Y., GAN, L.M., J. Nanosci. Nanotechnol., **4**, 2004, p. 197
15. BOUNOR-LEGARE, V., ANGELLOZ, C., BLANC, P., CASSAGNAU, P., MICHEL, A., Polymer, **45**, 2004, p. 1485
16. RUNA, M.T., WU, S.Z., ZHANG, D.Y., WU, G., Mat. Chem. Phys., **105**, 2007, p. 341
17. ZHONGLI, L., SHUXIAN, B., Mat. Lett., **61**, 2007, p. 3531
18. JANG, J., BAE, J., J. of Non-Cryst. Solids., **352**, 2006, p. 3979
19. YILMAZ, E., RAMSTRÖM, O., MÖLLER, P., SANCHEZ, D., MOSBACH, K., J. Mat. Chem., **12**, 2002, p. 1577
20. ZHANG, W., WANG, H., JIN, Z., Mat. Lett., **59**, 2005, p. 250
21. PAVARAJARN, V., KIMURA, S., J. Am. Ceram. Soc., **84**, 2001, p. 1669
22. GUNDIAH, G., MADHAV, G. V., GOVINDARAJ, A., SEIKH, M.M., RAO, C., J. Mat. Chem., **12**, 2002, p. 1606

Manuscript received: 7.09.2009